



# Adaptive High-Order Methods for Nonlinear Stokes Problems Arising in Mantle Flow

Carsten Burstedde<sup>§</sup>, Omar Ghattas<sup>\*†</sup>, Michael Gurnis<sup>‡</sup>, Tobin Isaac<sup>\*</sup>, Johann Rudi<sup>\*</sup>, Georg Stadler<sup>\*</sup>, Hari Sundar<sup>\*</sup>

<sup>\*</sup>Institute for Computational Engineering and Sciences (ICES), The University of Texas at Austin  
<sup>†</sup>Jackson School of Geosciences and Department of Mechanical Engineering, The University of Texas at Austin  
<sup>‡</sup>Seismological Laboratory, California Institute of Technology, Pasadena, California  
<sup>§</sup>Institut für Numerische Simulation, Universität Bonn, Germany



## Summary

- Our target is the efficient, accurate and scalable solution of large-scale nonlinear Stokes systems arising in the simulation of mantle flow with associated plate tectonics.
- Use Newton's method for the nonlinear Stokes system and preconditioned Krylov methods for the solution of the linearized systems.
- The discretization is based on adaptively refined meshes to resolve the strong variations in the viscosity, and a stable high-order velocity-pressure pair with discontinuous pressure functions to guarantee local mass conservation.
- Efficient solvers are particularly important for inverse problems in mantle flow, which require the repeated solution of large-scale nonlinear and linearized Stokes problems.

## 1. Mantle flow

Mantle convection is the thermal convection in the Earth's upper ~3000 km. It controls the thermal and geological evolution of the Earth and drives plate motion and mountain building. Mantle flows are driven by the hot core and radioactive decay in the mantle itself.

### Model equations

Rock in the mantle moves like a viscous, incompressible fluid on time scales of millions of years. From conservation of mass and momentum, we obtain that the flow velocity can be modeled as a **nonlinear Stokes** system:

$$-\nabla \cdot [\mu(T, \mathbf{u})(\nabla \mathbf{u} + \nabla \mathbf{u}^T)] + \nabla p = \text{Ra} T \mathbf{e}_r \quad (\text{S1})$$

$$\nabla \cdot \mathbf{u} = 0 \quad (\text{S2})$$

- $T$  ... temperature
- $\mathbf{u}$  ... velocity
- $p$  ... pressure
- $\mu(T, \mathbf{u})$  ... viscosity
- $\text{Ra} \sim 10^6 - 10^9$  ... Rayleigh number
- $\mathbf{e}_r$  ... radial direction

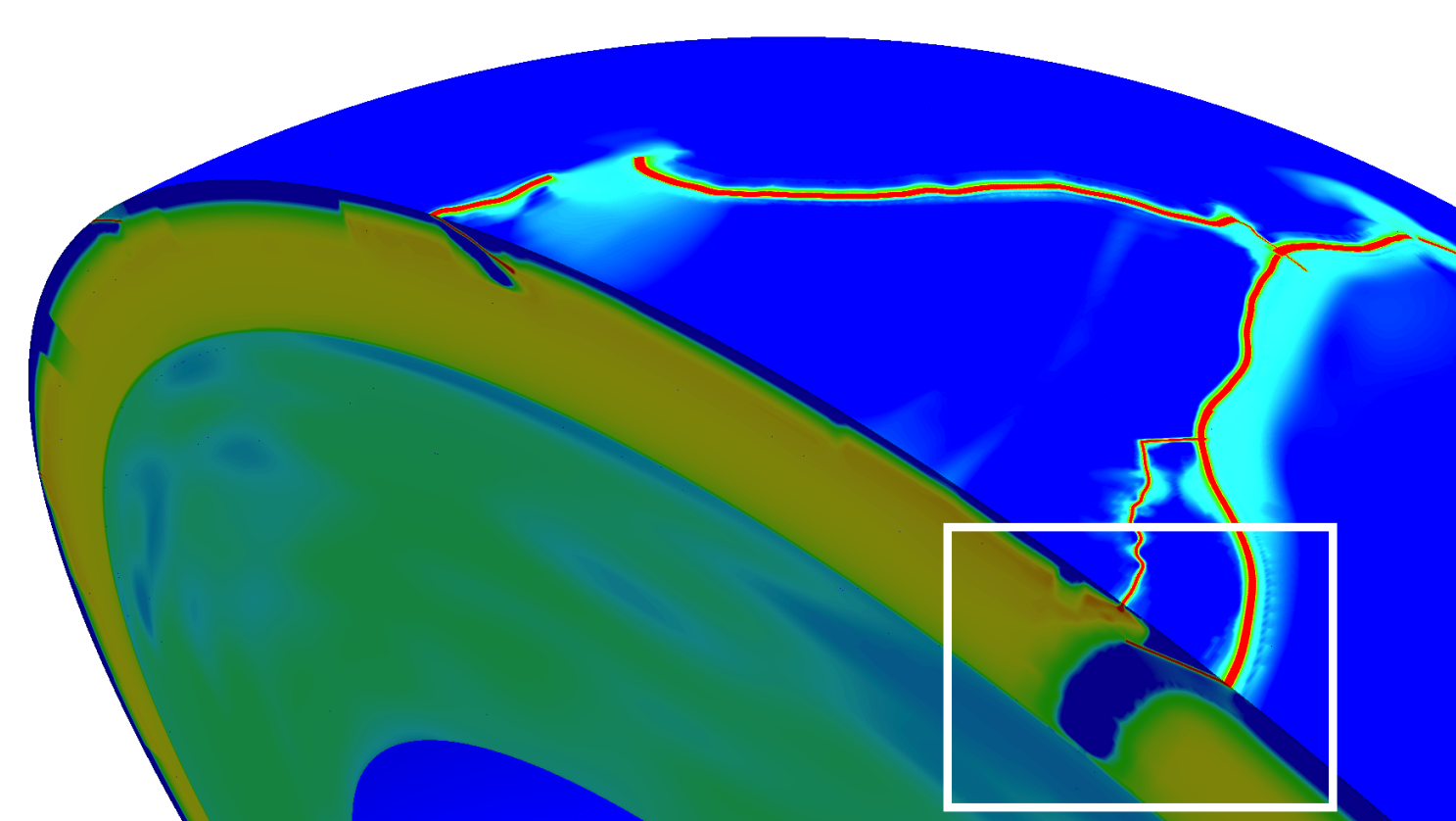
The temperature and strain-rate dependent viscosity is commonly described by the following rheology:

$$\mu(T, \mathbf{u}) = \mu(T) \mu(\mathbf{u}) = e^{E_a(0.5-T)} (\dot{\epsilon}_{II}(\mathbf{u}))^{\frac{n-1}{n}},$$

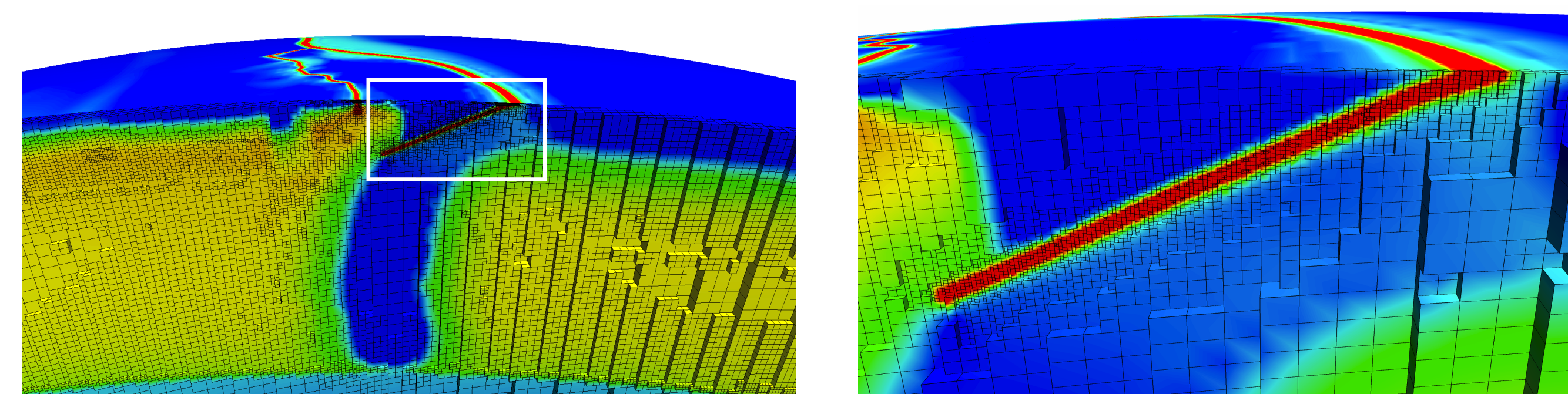
$\dot{\epsilon}_{II}$  is the second invariant of the strain rate tensor,  $E_a$  the activation energy, and  $n \geq 1$ .

### Solver challenges

- Variation of viscosity  $\mu$  by up to 8 orders of magnitude.
- Highly localized features w.r.t. Earth radius ~6371 km: plate thickness ~50 km and shearing zones at plate boundaries ~5–10 km.
- Desired resolution of ~1 km would result in  $O(10^{12})$  degrees of freedom on a uniform mesh of Earth's mantle.



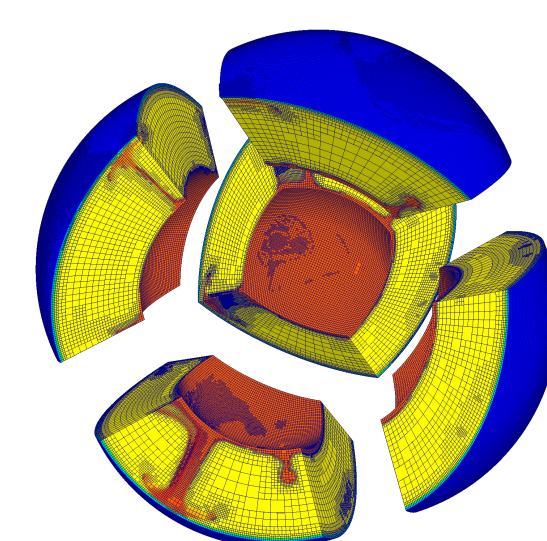
(Visualization by L. Alisic)



## 2. Adaptive, high-order finite element discretization

### Parallel octree-based AMR using the *p4est* library

- Hexahedral meshes with non-conforming elements.
- Parallel adaptive mesh refinement and coarsening.
- Octree algorithms enable fast neighbor search, repartitioning, and 2:1 balancing.
- Scalable to at least hundreds of thousands of processors.



## Finite element discretization

- We use high-order velocity-pressure pairings in  $(\mathbb{Q}_N)^3 \times \mathbb{P}_{N-1}^{\text{disc}}$  or  $(\mathbb{Q}_N)^3 \times \mathbb{Q}_{N-2}^{\text{disc}}$ , which satisfy the inf-sup conditions for conforming and non-conforming meshes.
- Algebraic constraints on element faces with hanging nodes enforce continuity of the global velocity basis functions.
- Hexahedral elements allow for the basis functions derivatives to be calculated efficiently using tensor products.
- Fast, matrix-free application of stiffness and mass matrices.

## 3. Large-scale parallel Stokes solver

### Nonlinear solver: Inexact Newton-Krylov method

Given an iterate  $(\mathbf{u}, p)$ , the Newton update  $(\tilde{\mathbf{u}}, \tilde{p})$  for the Stokes system (S1), (S2) solves the PDE

$$-\nabla \cdot [\mu'(T, \mathbf{u})(\nabla \tilde{\mathbf{u}} + \nabla \tilde{\mathbf{u}}^T)] + \nabla \tilde{p} = -\mathbf{r},$$
$$\nabla \cdot \tilde{\mathbf{u}} = -r.$$

$\mathbf{r}$  and  $r$  are residuals and  $\mu'(T, \mathbf{u})$  is an anisotropic 4th-order tensor given by

$$\mu'(T, \mathbf{u}) = \mu(T) \mu(\mathbf{u}) \left( \mathbf{I} - \frac{n-1}{n} \frac{(\nabla \mathbf{u} + \nabla \mathbf{u}^T) \otimes (\nabla \mathbf{u} + \nabla \mathbf{u}^T)}{\dot{\epsilon}_{II} + \varepsilon} \right),$$

where  $0 < \varepsilon \ll 1$  is a regularization parameter and  $\mathbf{I}$  the 4th-order identity tensor. The next Newton iterate is  $(\alpha > 0)$  is the step size:

$$(\mathbf{u}_{\text{new}}, p_{\text{new}}) = (\mathbf{u}, p) + \alpha(\tilde{\mathbf{u}}, \tilde{p}).$$

- Newton update is computed inexactly via Krylov subspace iterative method.
- Krylov tolerance decreases with subsequent Newton steps to guarantee superlinear convergence.
- Line search in direction  $(\tilde{\mathbf{u}}, \tilde{p})$  is conducted using the weak Wolfe conditions to ensure reduction of residuals.

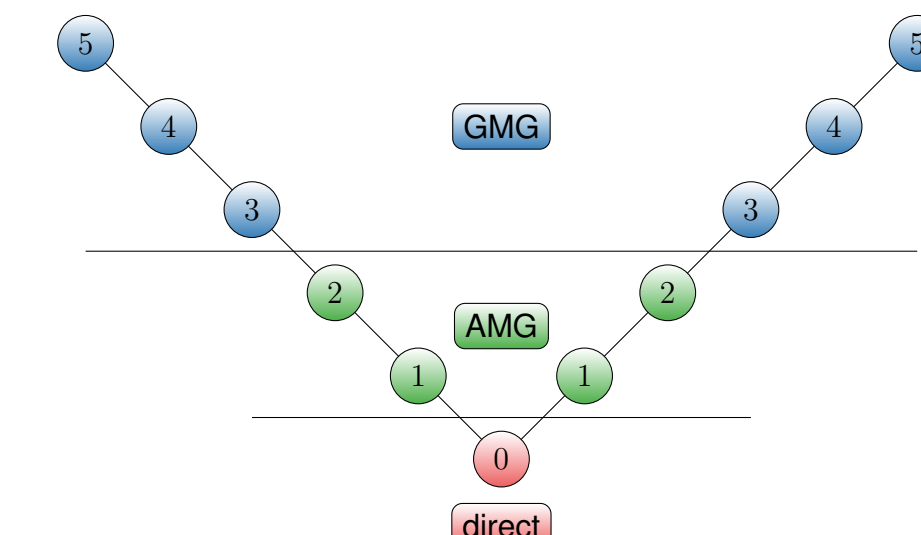
### Linear solver: Preconditioned Krylov method

- Krylov method: Upper triangular block preconditioned GMRES (GMRES from *PETSc*).
- Schur complement preconditioner that can be written as a matrix consisting of two blocks: (1) viscous block and (2) pressure Schur complement.
- The pressure Schur complement is approximated by a spectrally equivalent lumped mass matrix weighted with the inverse viscosity, or by a BFBT approximation.
- Algebraic multigrid (AMG) V-cycle (*Trilinos ML*) with SOR smoother (*PETSc*) approximates the viscous block.
- AMG is called with a linearized version of the stiffness matrix, i.e., the high-order discretization is sparsified using trilinear elements based on the high-order degrees of freedom. This results in faster matrix assembly for *Trilinos ML* and is more suitable for AMG.

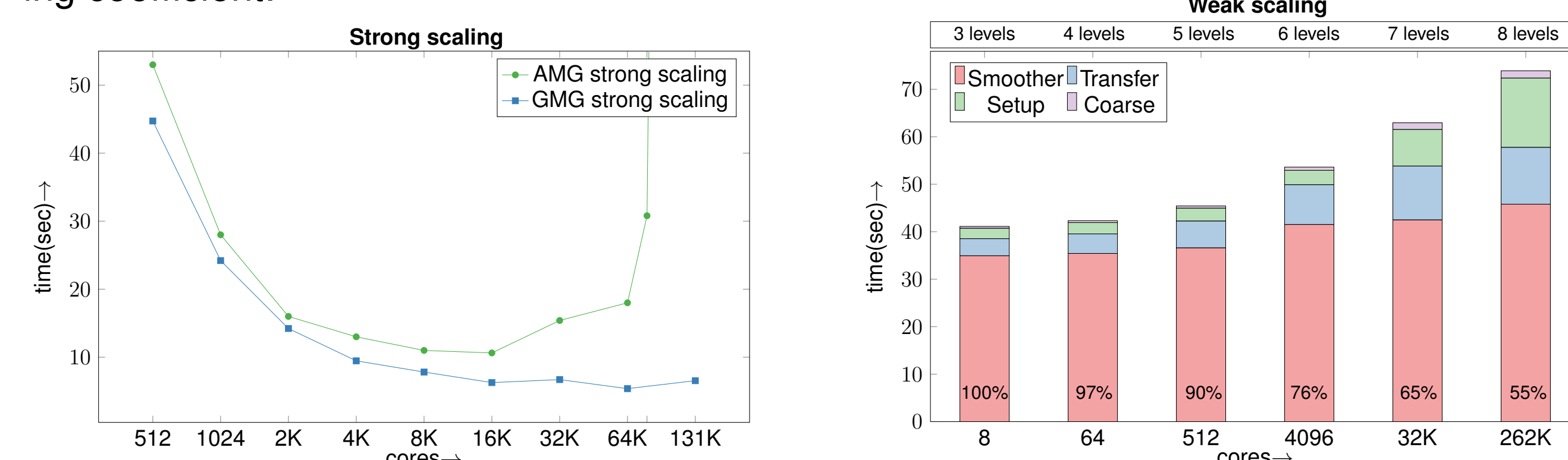
### Parallel, hybrid geometric-algebraic multigrid for the viscous block

We will replace AMG with our new hybrid geometric-algebraic multigrid solver, which has better scalability properties compared to *Trilinos ML* due to its mesh-based hierarchy setup.

- GMG-AMG approach matches geometric decomposition of the domain.
- AMG is used for small problem sizes on small process counts.
- Smoothed aggregation algebraic multigrid (*Trilinos ML*).



Scalability results for 3D Poisson problem on spherical domain with isotropic spatially varying coefficient:



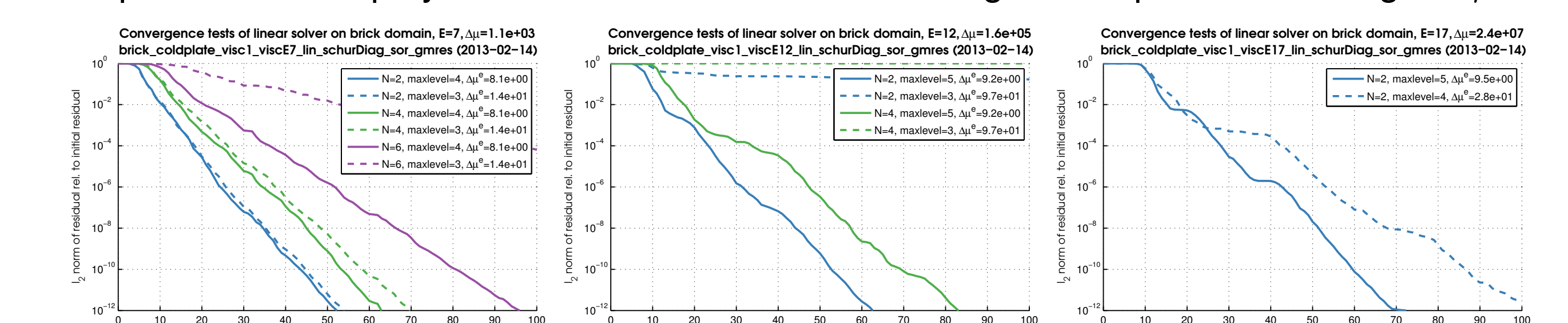
124M elements, 5 GMG levels, AMG for coarse solve, 1 MPI process per core, Jaguar XK6.

## 4. Linear and nonlinear convergence

We consider two test problems on a rectangular domain. Prior to invoking the solver, the meshes were adaptively refined to resolve the variations in viscosity. The element pairing  $(\mathbb{Q}_N)^3 \times \mathbb{P}_{N-1}^{\text{disc}}$  is used for all tests. Further, we define the global viscosity variation  $\Delta\mu = \max(\mu) / \min(\mu)$  and the viscosity variation per element  $\Delta\mu^e = \max(\mu^e) / \min(\mu^e)$ .

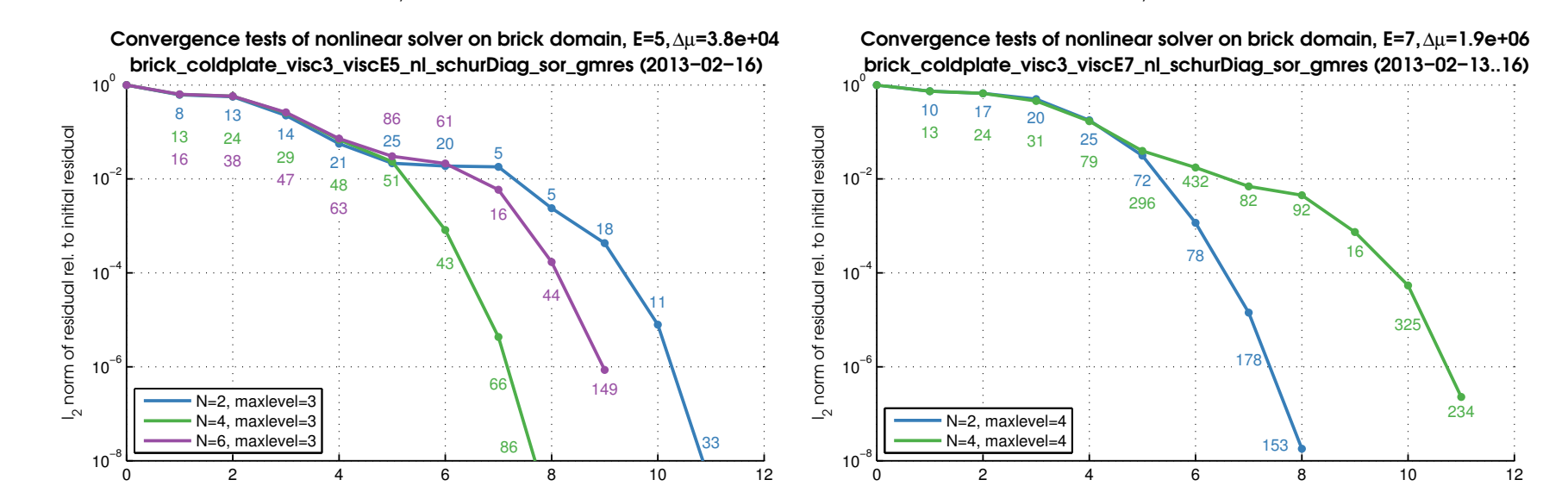
### Convergence for single plate problem, plate thickness ~130 km

**Linear solver:** Convergence results for  $N = 2, 4, 6$ , and viscosity variation per element  $\Delta\mu^e \leq 10$  (solid lines) and  $\Delta\mu^e \leq 100$  (dashed lines). Different figures represent different global viscosity variations  $\Delta\mu \sim 10^3, 10^5, 10^7$ . Note that the convergence behavior is rather independent of the polynomial order and that the convergence is poor for the larger  $\Delta\mu^e$ .

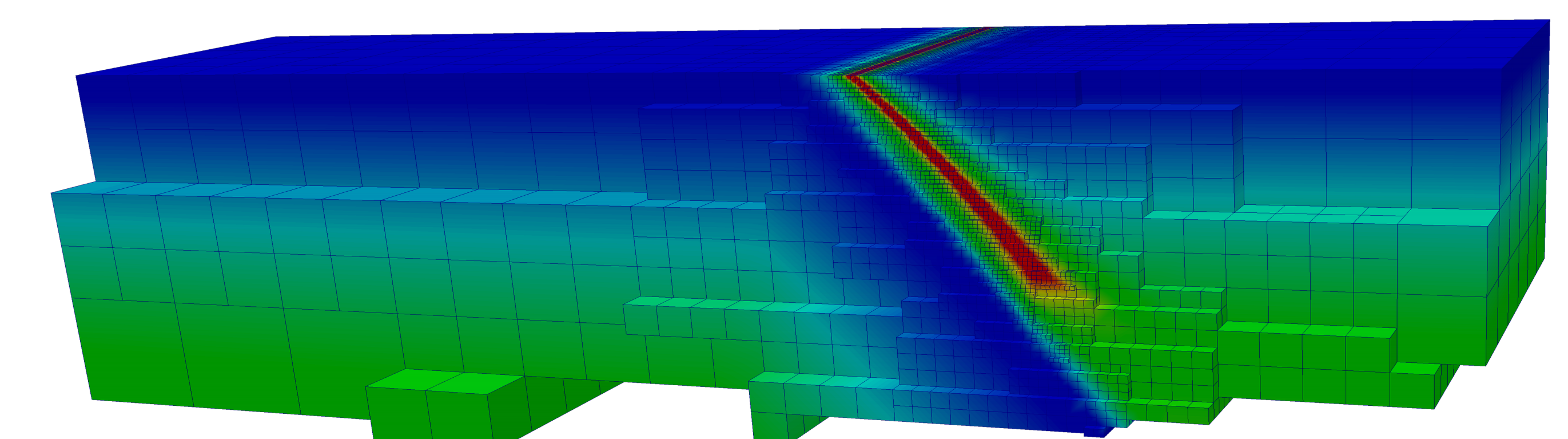


### Nonlinear solver:

Convergence results with initial  $\Delta\mu^e \leq 10$ . Global viscosity variations of solution are  $\Delta\mu \sim 10^4$  (left) and  $\Delta\mu \sim 10^6$  (right).



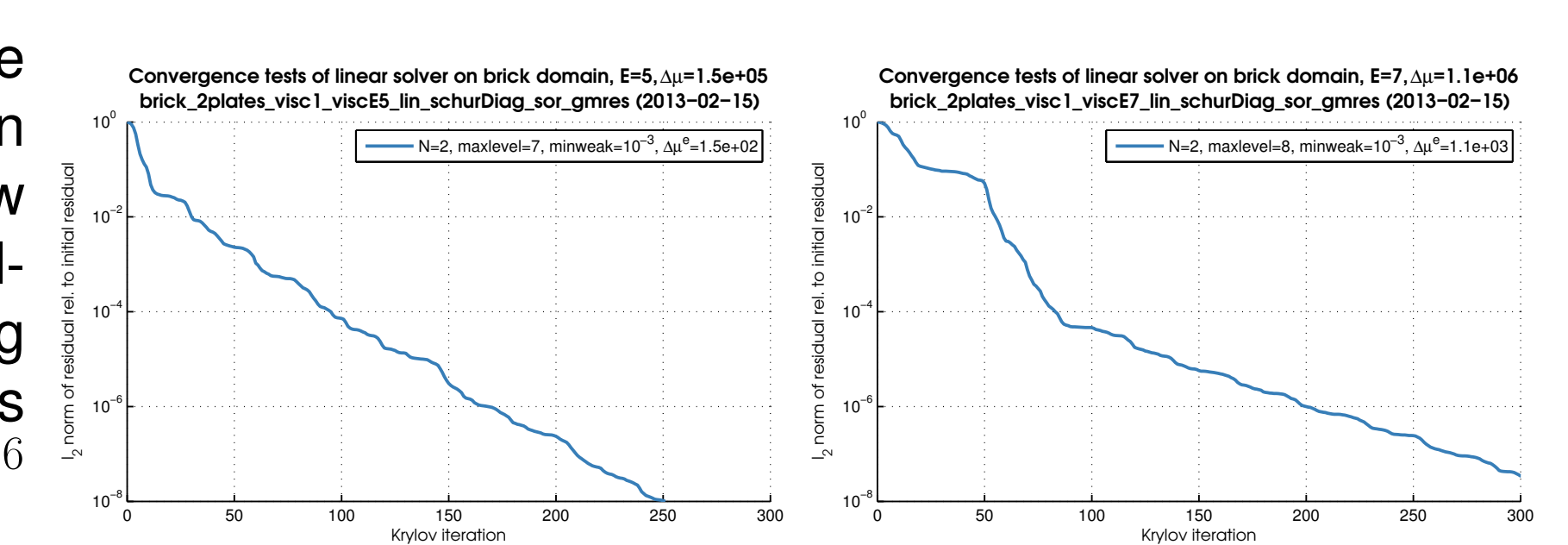
### Convergence for slabs problem with subducting & overriding plate



The extraction from the mesh (above) shows the initial adaptive refinement to resolve the variations in the viscosity. The shearing zone between the plate boundaries of subducting plate and overriding plate is modeled by reducing the viscosity by several orders of magnitude.

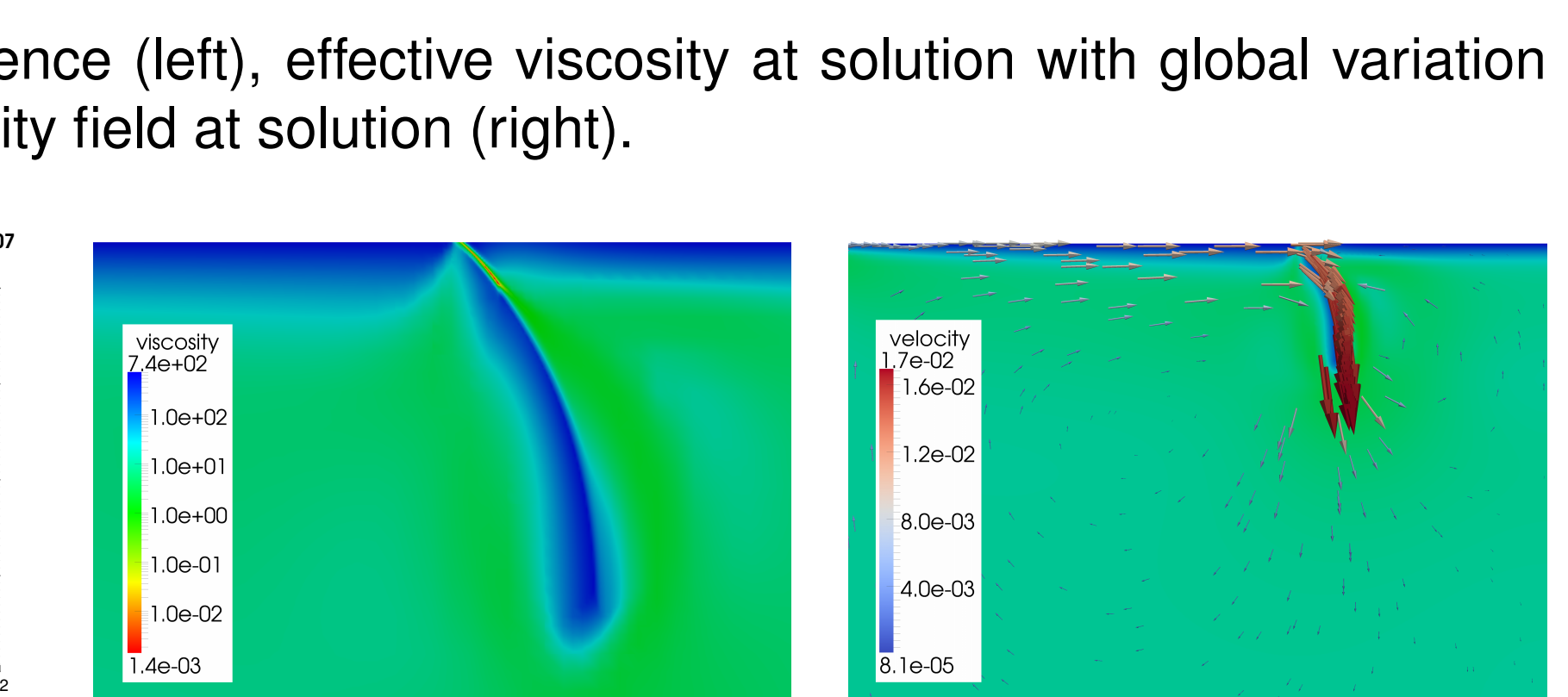
### Linear solver:

Convergence for  $N = 2$ ; the viscosity in the plate boundary (narrow red zone) is reduced by multiplication with  $10^{-3}$ , leading to global viscosity variations  $\Delta\mu \sim 10^5$  (left) and  $\Delta\mu \sim 10^6$  (right).



### Nonlinear solver:

Convergence (left), effective viscosity at solution with global variation  $\Delta\mu \sim 10^7$  (middle), and velocity field at solution (right).



### Acknowledgement

Support through the NSF CDI program (CMMI-1028889, CMMI-1028978, OPP-0941678) is gratefully acknowledged.